Analytical Sciences (2024) 40:141–149
https://doi.org/10.1007/s44211-023-00436-z

ORIGINAL PAPER

Surface characterization and electroanalytical applications of the newly developed copper(II)-selective potentiometric sensor

Oguz Özbek[1] · Onur Cem Altunoluk[2] · Ömer Isildak[2]

Received: 21 August 2023 / Accepted: 25 September 2023 / Published online: 12 October 2023

Abstract

In this work, we developed a new copper(II)-selective potentiometric sensor and investigated its surface with scanning electron microscopy (SEM). Besides the surface images of the sensors conditioned in copper(II) solutions, energy–dispersive X-ray (EDX) and mapping studies were carried out. According to the results obtained, it was determined that copper(II) ions adhered to the porous areas on the sensor surface, and that Cu^{2+} ions showed a wide distribution on the sensor surface in mapping studies. The new sensor had a Nernstian response of 29.3 ± 0.5 mV/decade in the concentration range of 1.0×10^{-1}–1.0×10^{-5} M and a low detection limit of 8.56×10^{-6} M. The proposed sensor had fast response time (< 10 s), wide pH working range (5.0–10.0), good repeatability and stability. Finally, the sensor performed the determination of copper(II) ions in various water samples with very high recoveries (96.0–102.0%).

Keywords Scanning electron microscopy · Copper · Heavy metal · Sensor

Introduction

Potentiometric ion-selective electrodes (ISEs) have been recently highly promoted owing to their high selectivity, good repeatability, fast response, simple operation, and low cost [1–3]. Among the different potentiometric sensors, solid contact ion-selective sensors are the most preferred [4]. Polymeric membrane ISEs have become an attractive analytical tool in industrial, environmental, agricultural analyses, process control, medicinal drug, and food analysis due to their significant advantages [5–7].

Heavy metals are toxic to many organisms above a threshold concentration and therefore the determination of heavy metal ions in various samples is highly important [8]. Copper (Cu), a heavy metal, is widely used in industry due to its chemical stability, electrical conductivity and ability to form alloys with many metals [9, 10]. Copper is considered to be the second most toxic metal to aquatic life, and leaches into waters through wastewater from its various industries, posing a high risk to public health [11]. Copper is also an essential trace element for living things and performs important biochemical functions in biological systems. However, excessive copper levels are toxic and can cause various diseases in humans [12–15]. So far, copper has been determined in various samples using analytical techniques such as inductively coupled plasma–optical emission spectroscopy (ICP–OES), flame atomic absorption spectrometry (FAAS), high performance liquid chromatography (HPLC), ion chromatography, UV–Vis spectrometry and cyclic voltammetry [16–20]. Generally, these methods require experienced personnel and well-equipped laboratories as they require complex analytical procedures. In addition, they are expensive instruments and are not suitable for use in field analysis [21, 22].

The SEM is an important tool widely used to study the topology and elemental composition of sample surfaces, allowing researchers to study the surface structure of many material types in detail [23]. SEM is widely used to analyze the surface morphology of sensors and to determine the percentage of each element present on the surface. It is also used to link the potentiometric response to surface morphology and to correlate surface morphology with the response obtained [24, 25].

✉ Oguz Özbek
oguz.ozbek@beun.edu.tr

[1] Science and Technology, Application and Research Center, Zonguldak Bülent Ecevit University, 67600 Zonguldak, Turkey

[2] Department of Chemistry, Faculty of Science and Arts, Tokat Gaziosmanpaşa University, 60250 Tokat, Turkey

In this paper, we report the development of a novel selective and sensitive potentiometric sensor using 1-(3-carboxyphenyl)-2-thiourea (Fig. 1) for the determination of Cu(II) ions. The analytical performance of the newly developed sensor, including the linear concentration range, detection limit, selectivity, repeatability, and pH working range was evaluated. In addition, the surface images of the sensors conditioned in Cu(II) solution for 1 h were examined by SEM technique.

Experimental

Chemicals and reagents

1-(3-Carboxyphenyl)-2-thiourea was used as an ionophore and was purchased from Sigma Aldrich. Graphite, epoxy (Macroplast Su 2227) and hardener (Desmodur RFE) used in the preparation of conductive solid contact electrodes were purchased from Sigma Aldrich, Henkel (Istanbul, Turkey) and Bayer AG (Darmstadt, Germany), respectively. High molecular weight poly(vinyl chloride) (PVC), plasticizers [bis (2-ethylhexyl) adipate (DEHA), dibutyl phthalate (DBP), *o*-nitrophenyloctylether (*o*-NPOE), and bis(2-ethylhexyl)sebacate (BEHS)], potassium tetrakis (*p*-chlorophenyl) borate (KT*p*ClPB) and tetrahydrofuran (THF) used in the preparation of copper(II)-selective potentiometric sensors were obtained from Sigma Aldrich. Nitrate salts of all metals used in selectivity studies were purchased from Sigma Aldrich, Merck, and Fluka. Nitric acid (HNO_3) and sodium hydroxide (NaOH) used for pH adjustments were purchased from Merck.

Apparatus

Surface characterization, energy-dispersive X-ray (EDX) and mapping analyses of copper(II)-selective potentiometric sensors were carried out with a scanning electron microscope (Quanta FEG 450-FEI). All potential measurements were performed using a multi-channel potentiometer (Medisen Medical Ltd. Sti., Turkey). A silver/silver chloride electrode (Ag/AgCl, 3 M KCl) was used as the reference electrode (Thermo Scientific Orion 900100). All solutions were freshly prepared using the human ultrapure water system (Zeneer Power I, 18.2 MΩ cm^{-1}).

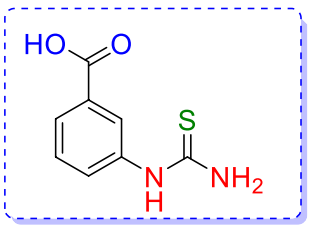

Fig. 1 The chemical structure of 1-(3-carboxyphenyl)-2-thiourea

Method

Preparation of copper(II)-selective potentiometric sensors

Conductive solid contact PVC membrane potentiometric sensors were prepared in two stages as previously reported in the literature [26]. First, solid contact electrodes were prepared by homogeneously dissolving graphite (50.0%), epoxy (35.0%) and hardener (15.0%) in THF (approximately 3 mL). The hardener in the solid contact composition is an aromatic polyisocyanate component. 15 cm long copper wires were dipped into this mixture approximately 3–4 times and left to dry in a dark medium for 24 h. Then, to prepare polymer membrane copper(II)-selective sensors, ionophore, plasticizer, PVC and KT*p*ClPB were dissolved in THF (approximately 3 mL) in the ratios given in Table 1, and mixed until a certain viscosity was reached. The pre-prepared solid contact electrodes were dipped into this mixture several times and their surfaces were coated. The prepared PVC membrane copper(II)-selective potentiometric sensors were left to dry for approximately 12 h.

Potential measurements

The prepared sensors were used directly without any conditioning. The potential measurements were carried out at 25 ± 1.0 °C using an Ag/AgCl reference electrode with the following cell assembly:

$$\mathrm{Ag/AgCl;\ KCl\ (3M)} \,\|\, \mathrm{Cu^{2+}\ sample\ solution}$$

$$\mid \mathrm{Cu^{2+}\ -\ selective\ membrane} \mid \mathrm{Solid\ contact} \mid \mathrm{Cu\ wire.}$$

The copper(II) solutions were prepared by subsequent dilution from 1.0×10^{-1} M stock solutions of $Cu(NO_3)_2$. ISEs calibrations were performed in the concentration range from 1.0×10^{-5} to 1.0×10^{-1} M Cu^{2+} ions.

Results and discussion

Membrane optimization

In this study, sensors with ten different compositions were prepared using different ratios of ionophore, plasticizer, PVC and KT*p*ClPB. The potentiometric performance characteristics of the prepared sensors such as linear concentration range, detection limit and slope (mV/decade) were tested. When the potentiometric performance

Table 1 Prepared sensor components and performance characteristics

No	Membrane composition (*w*/*w*)							Potentiometric performance			
	PVC	Ionophore	Plasticizer				KT*p*ClPB	Linear concentration range (M)	Limit of detection (M)	Slope (mV/decade)	R^2
			DEHA	BEHS	DBP	*o*-NPOE					
1	32.0	3.0	64.0				1.0	1.0×10^{-1}–1.0×10^{-5}	8.68×10^{-6}	23.5 (± 3.0)	0.9899
2	32.0	3.0		64.0			1.0	1.0×10^{-1}–1.0×10^{-4}	2.71×10^{-5}	12.4 (± 1.5)	0.9781
3	32.0	3.0			64.0		1.0	1.0×10^{-1}–1.0×10^{-5}	9.72×10^{-6}	24.2 (± 2.0)	0.9776
4	32.0	3.0				64.0	1.0	1.0×10^{-1}–1.0×10^{-4}	9.64×10^{-5}	19.0 (± 3.0)	0.9882
5	31.0	2.0			66.0		1.0	1.0×10^{-1}–1.0×10^{-5}	9.44×10^{-6}	23.7 (± 2.1)	0.9872
6	30.0	4.0	65.0				1.0	1.0×10^{-1}–1.0×10^{-5}	9.69×10^{-6}	23.0 (± 1.5)	0.9876
7	29.0	5.0	65.0				1.0	1.0×10^{-1}–1.0×10^{-5}	8.56×10^{-6}	29.3 (± 0.5)	0.9975
8	29.0	5.0		65.0			1.0	1.0×10^{-1}–1.0×10^{-5}	9.79×10^{-6}	24.0 (± 3.4)	0.9891
9	29.0	5.0			65.0		1.0	1.0×10^{-1}–1.0×10^{-5}	9.47×10^{-6}	23.7 (± 3.1)	0.9825
10	29.0	5.0				65.0	1.0	1.0×10^{-1}–1.0×10^{-4}	2.88×10^{-5}	33.9 (± 2.5)	0.9787

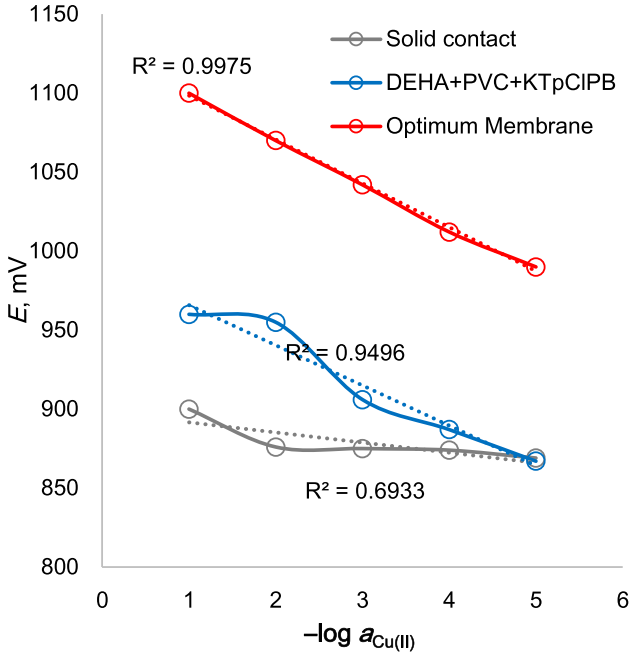

Fig. 2 The effect of the ionophore on the potential response of the sensor

characteristics were evaluated, it was determined that the mixture containing 5.0% ionophore in its composition had the lowest detection limit and Nernstian response compared to other sensors (Table 1). According to the potentiometric performance characteristics in Table 1, DEHA was determined to be the most suitable plasticizer among sensors containing 5% ionophore compared to other plasticizers. Thus, the optimum membrane composition was determined as 5.0% ionophore, 65.0% DEHA, 29.0% PVC and 1.0% KT*p*ClPB.

Influence of the ionophore

To demonstrate the interaction of the ionophore with the analyte ion, the potential change of the electrode without ionophore and the solid contact electrode against copper(II) ions was examined. Figure 2 shows that electrodes without ionophores exhibit a non-linear behavior towards copper(II) ions. As a result, the ionophore used in the study interacts with copper(II) ions and exhibits an ideal potentiometric behavior.

The mechanism of copper(II) ions with the developed ion-selective sensor is summarized in Fig. 3. Here, a typical ion exchange occurs. The ionophore, which can directly interact with analyte ions in the PVC membrane, can trap copper ions at the interface between the solution and membrane phases. The transition of copper(II) ions between the solution phase and the membrane phase depends on its activity or concentration. Without the

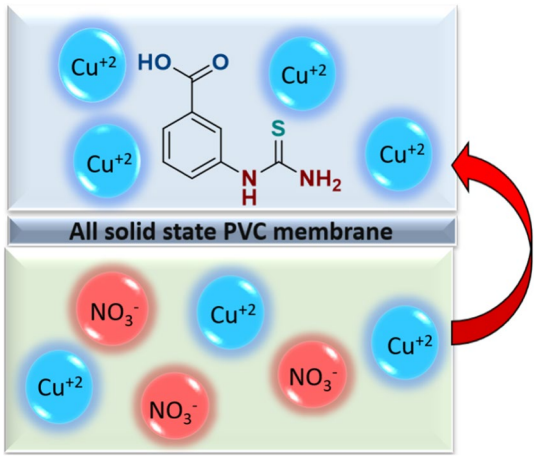

Fig. 3 Interaction mechanism of the sensor with copper(II) ions

ionophore, the analyte ion cannot pass through the membrane. If the concentrations at the solution-membrane interface are unequal, a phase-boundary potential occurs in the membrane. This potential is determined by adding a reference electrode to the potentiometric measurement system [27].

Investigation of the sensor surface with SEM technique

The surface images of the newly developed copper(II)-selective sensor were investigated using SEM technique. After the sensors were conditioned in Cu(II) solutions for 1 h, their surfaces were examined. In Fig. 4a, SEM and EDX images of the surface are given. In Fig. 4a, the SEM image was examined without selecting any region. In Fig. 4b, one of the white regions in the SEM image was marked and EDX analysis of this region was performed. In Fig. 4b, it is clearly seen that the whiteness collected in a hollow region belongs to copper(II) ions. As seen there, copper(II) ions are attached to the surface. Other atoms (C, O, Cl and S) in the EDX spectrum belong to the components in the PVC membrane structure. In Fig. 5, SEM images were taken at different magnifications and it was determined that the white dots were distributed homogeneously in the spaces on the sensor surface. In Fig. 6, the mapping study of the sensor surface is given. There, the atoms in the PVC membrane structure and the distribution of Cu(II) ions on the surface can be seen. Figure 6 shows that Cu(II) ions are located on the entire sensor surface. As a result, the retention of copper(II) ions on the sensor surface indicates that the ionophore used strongly interacts with Cu(II) ions.

The potentiometric response, calibration curve and repeatability

The potentiometric response of the sensor with optimum components is given in Fig. 7a. As can be seen in Fig. 7a, the sensor exhibited a Nernstian and ideal potentiometric response to copper(II) ions. The calibration curve of the sensor is presented in Fig. 7b. As seen in Fig. 7b, the sensor has a high R^2 value in the concentration range of 1.0×10^{-1}–1.0×10^{-5} M. The detection limit of the sensor was calculated using data presented in Fig. 5b. For this purpose, the value (986 mV) corresponding to the intersection of the horizontal and vertical axes was substituted in the linear equation below:

$$E = -27.587\left[-\log\left(Cu^{2+}\right)\right] + 1125.8.$$

The detection limit of the copper(II)-selective sensor was calculated as 8.56×10^{-6} M. The repeatability of the newly developed copper(II)-selective sensor was determined using copper(II) solutions with three different concentrations (10^{-2}, 10^{-3} and 10^{-4} M). As seen in Fig. 7c, the sensor exhibited a highly reproducible and stable potential response.

Response time

The response time of the sensor was determined according to the rules recommended by IUPAC [28]. After 7 s, an equilibrium potential was obtained (± 1.0 mV) indicating a very fast response time (< 10 s), as shown in Fig. 8. This shows that the sensor has a very fast response time from low to high concentration [29]. It was determined that the new copper(II)-selective sensor quickly equilibrated in less than 10 s for each tenfold concentration change.

pH working range

The effect of pH on the potential response of the newly developed sensor to Cu(II) ions was examined at two different concentrations of the standard Cu(II) solutions by varying the pH of the solutions from 2.0 to 12.0. For this purpose, pH adjustments were made using HNO_3 and NaOH solutions. 1.0×10^{-2} and 1.0×10^{-3} M Cu(II) solutions were added to the solutions, and subsequently the potential was measured. The pH working range of the sensor is given in Fig. 9. As can be seen in this figure, the sensor worked in the pH range of 5.0–10.0 at both concentrations without being affected by pH changes. High potentials at pH < 5.0 are due to the hydronium ion concentration, while low potentials at pH > 10.0 may be due to the formation of hydroxide compounds of copper.

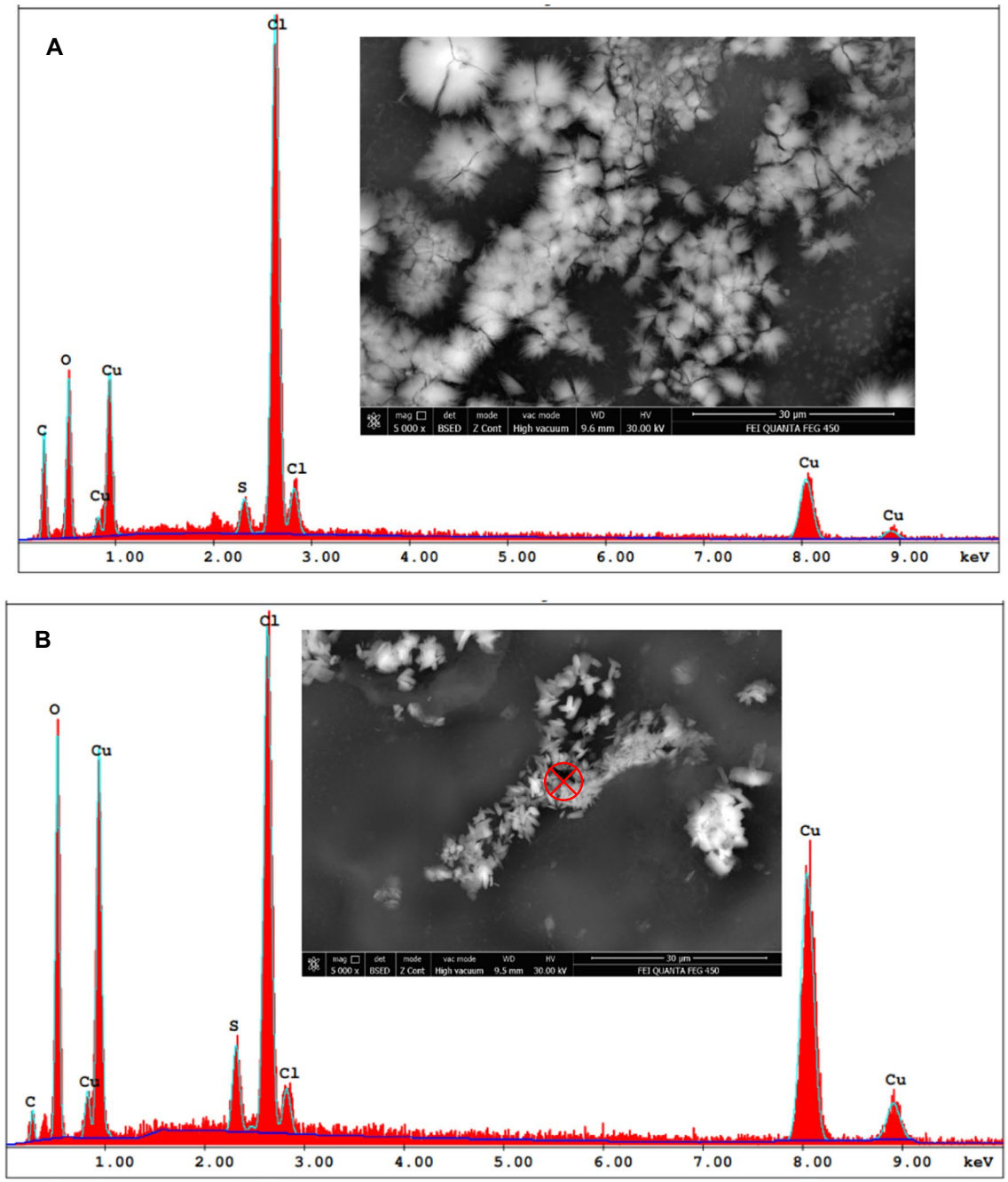

Fig. 4 **a**, **b** SEM and EDX analysis of the sensor conditioned in Cu(II) solution for 1 h

Potentiometric selectivity

The selectivity of the newly developed sensor was investigated using the separate solution method recommended by IUPAC [30]. The selectivity coefficients in Table 2 were calculated by substituting the potential values of the ions corresponding to the 1.0×10^{-2} M concentration in the equation below:

$$logK_{A,B}^{pot} = \frac{(E_B - E_A)Z_A F}{RTln10} + \left(1 - \frac{Z_A}{Z_B}\right) loga_A$$

where $K_{A,B}^{pot}$ is the selectivity coefficient, a_A is the activity of copper ion, a_B is the activity of interfering ion, z_A is the charge of copper ion, z_B is the charge of interfering ion; R, T, and F have the usual meanings.

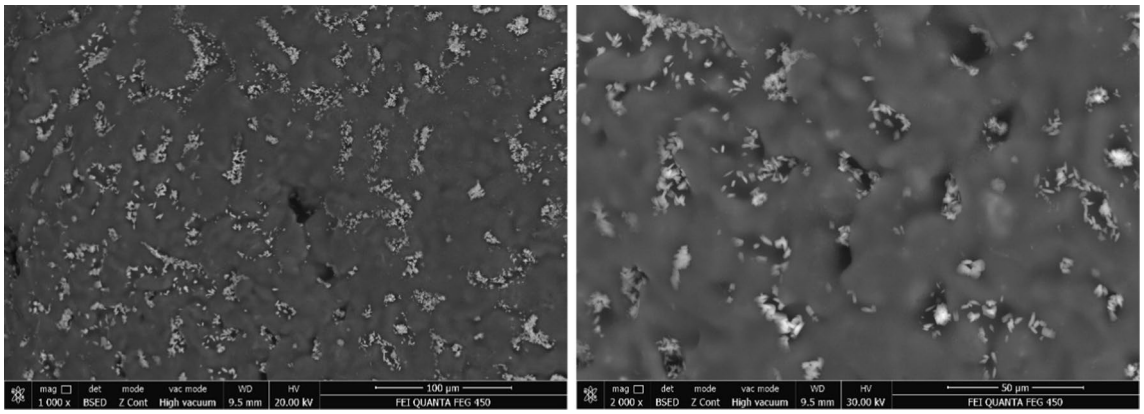

Fig. 5 Cu(II) ions attached to the gaps on the sensor surface

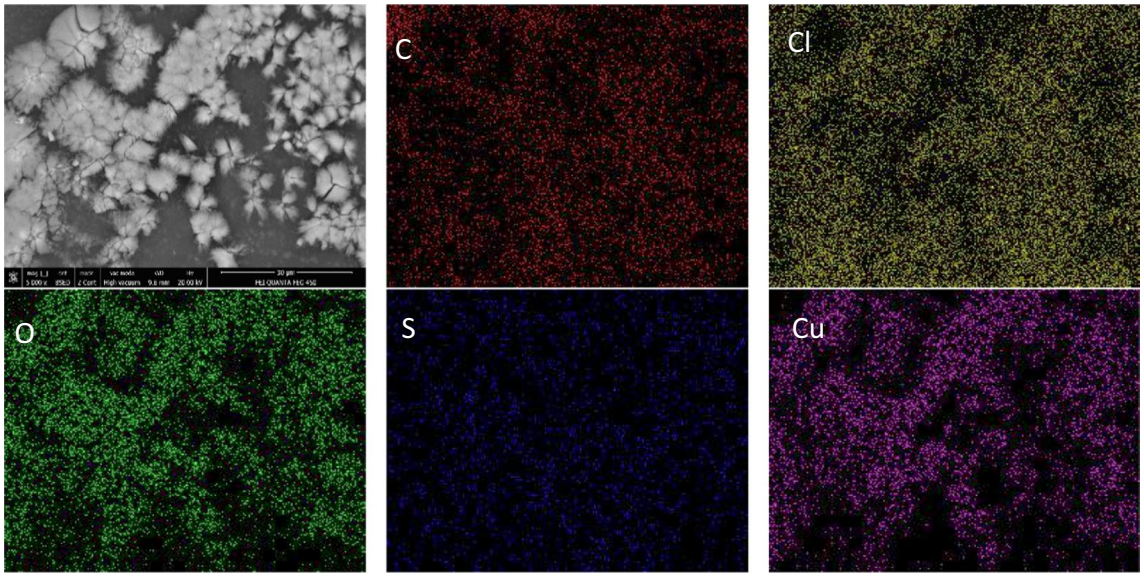

Fig. 6 Mapping analysis of the sensor conditioned in Cu(II) solution for 1 h

Table 2 Selectivity coefficients according to the separate solution method

Interfering ions	Selectivity coefficient $log\ K^{pot}_{Cu^{2+},M^{n+}}$	Interfering ions	Selectivity coefficient $log\ K^{pot}_{Cu^{2+},M^{n+}}$
Pb^{2+}	–0.65	Ba^{2+}	–2.20
Cr^{3+}	–0.89	Sr^{2+}	–2.28
Al^{3+}	–1.11	Ca^{2+}	–2.33
Zn^{2+}	–1.76	Ni^{2+}	–2.44
Co^{2+}	–1.89	Mg^{2+}	–2.71
Cd^{2+}	–2.06		

When Table 2 is examined, it is seen that the proposed new sensor exhibits good selectivity towards Cu(II) ions.

Real sample applications

The analytical applications of the newly developed sensor were determined using various water samples. Cu(II) ions

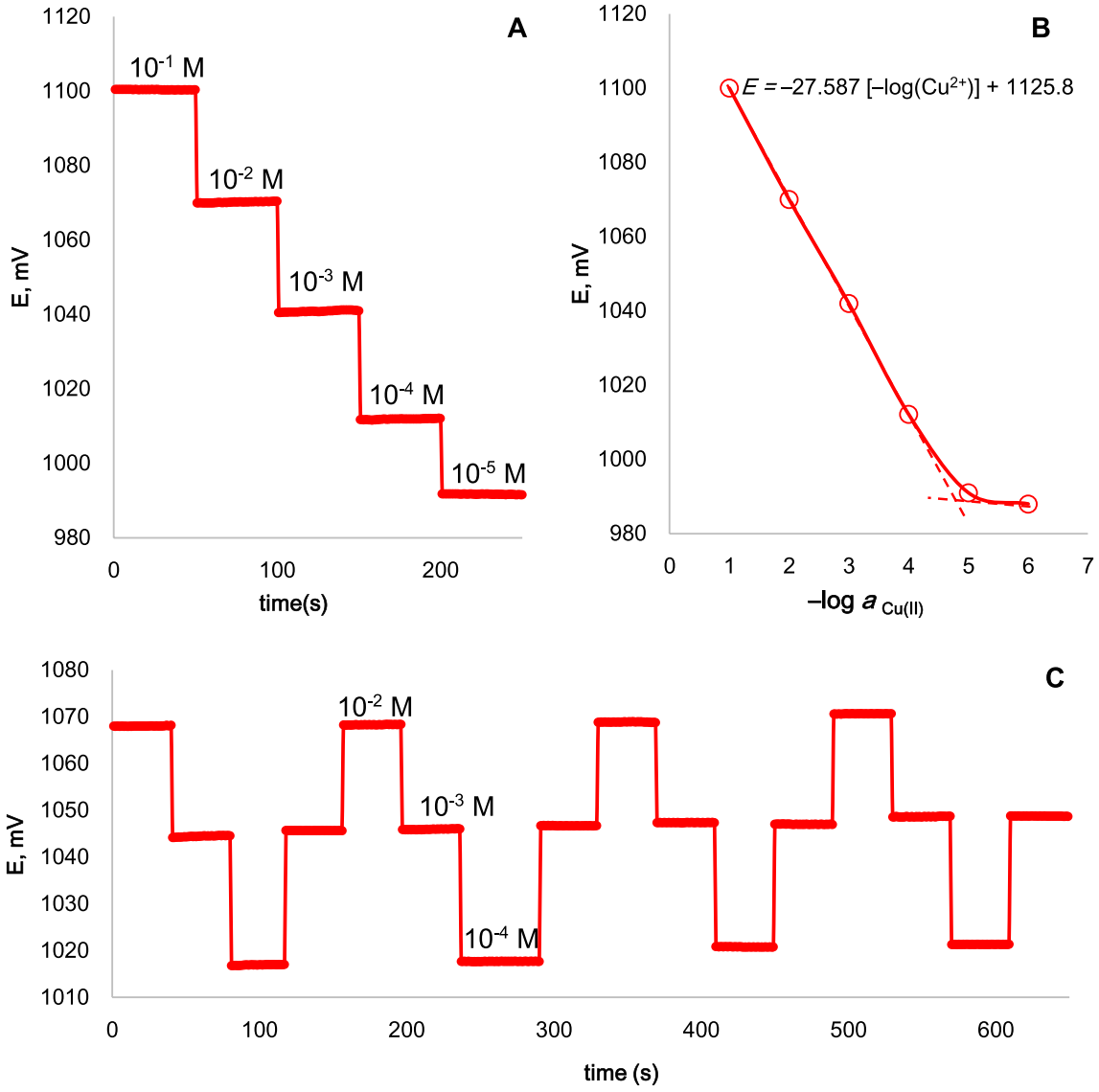

Fig. 7 **a** Potentiometric response. **b** calibration curve and **c** repeatability of newly developed copper(II)-selective sensor

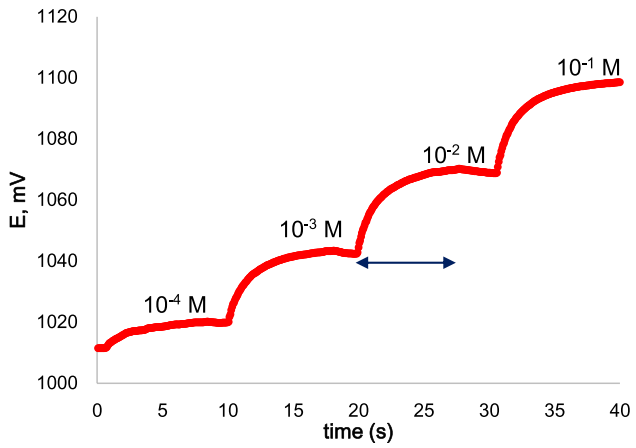

Fig. 8 Response time of newly developed copper(II)-selective sensor

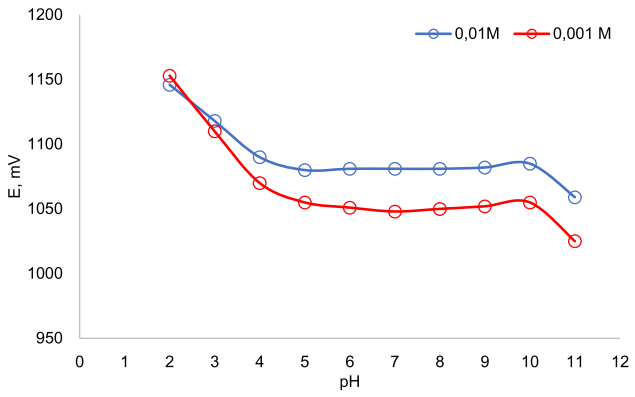

Fig. 9 pH working range of newly developed copper(II)-selective sensor

Table 3 The Cu(II) analysis in different water samples

Water samples	Cu^{2+} quantity, (M)		
	Added Cu^{2+}	Found (± SD) with sensor[a]	% Recovery
Purification drinking water	–	Not detection	–
	1.0×10^{-3}	$9.75\ (\pm0.29)\times10^{-4}$	97.5
Tap water (Kozlu, Turkey)	–	Not detection	–
	1.0×10^{-3}	$9.60\ (\pm0.35)\times10^{-4}$	96.0
Tap water (Zonguldak, Turkey)	–	Not detection	–
	1.0×10^{-3}	$1.02\ (\pm0.24)\times10^{-3}$	102.0
Bottled water	–	Not detection	–
	1.0×10^{-3}	$9.90\ (\pm0.10)\times10^{-4}$	99.0

[a]Average value ($n=3$)

Table 4 Comparison of the developed sensor with PVC membrane Cu(II)-ISE previously reported in the literature

Sensor composition	Concentration range (mol L^{-1})	Limit of detection (mol L^{-1})	Slope (mV/decade)	pH working range	Response time (s)	References
3.0% 1-phenyl-2-(2-hydroxyphenylhydrazo) butane-1,3-dione, 61.0% DBP, 30.0% PVC, 6.0% oleic acid	2.0×10^{-6}–5.0×10^{-3}	6.3×10^{-7}	28.8	3.0–8.0	10	[9]
4.0% ion imprinted polymer, 35.0% DBP, 61.0% PVC	1.0×10^{-5}–1.0×10^{-1}	2.0×10^{-6}	28.1	3.0–8.0	22	[31]
5.0% bis(2-hydroxybenzaldehyde)-1,2-diaminoethane, 61.0% DBP, 30.0% PVC, 5.0% NaTPB	5.0×10^{-4}–5.0×10^{-2}	3.9×10^{-4}	29.9	2.5–5.0	≈10	[32]
2.0% N,N′-bis(salicylidene)-1,3-diaminopropane, 68.0% *o*-NPOE, 29.75% PVC, 0.25% KT*p*ClPB	1.0×10^{-5}–1.0×10^{-2}	6.31×10^{-6}	30.4 ± 0.5	5.0	5–10	[33]
1.0% copper ionophore I, 65.7% DOS, 32.9% PVC, 0.86% NaTFPB	1.0×10^{-4}–1.0×10^{-2}	Not reported	29.05 ± 0.3	Not reported	10–50	[34]
5.0% 5,5′-(1,4-phenylene) bis(1,3,4-oxadiazol-2-amine), 62.0% DEHA, 32.0% PVC, 1.0% KT*p*ClPB	1.0×10^{-5}–1.0×10^{-1}	4.64×10^{-6}	42.2 ± 3.5	4.0–8.0	10	[35]
5.0% 1-(3-carboxyphenyl)-2-thiourea, 65.0% DEHA, 29.0% PVC and 1.0% KT*p*ClPB	1.0×10^{-5} –1.0×10^{-1}	8.55×10^{-6}	29.3 ± 0.5	5.0–10.0	< 10	This work

NaTPB sodium tetraphenylborate, *NaTFPB* sodium tetrakis[3,5-*bis*(*trifluoromethyl*)*phenyl*]borate

were added to the water samples at the rates in Table 3. Then, Cu(II) ion analysis was performed in the samples with the developed sensor. When Table 3 is examined, the newly developed sensor can detect copper ions in various water samples with high recoveries.

Comparison study

The potentiometric performance characteristics (concentration range, detection limit, slope, pH working range and response time) of the copper(II)-selective sensor are compared in Table 4 with other PVC membrane Cu(II)-ISEs reported in the

literature. As seen in Table 4, the proposed sensor has a better concentration range and lower detection limit than some of the copper(II)-selective sensors proposed in recent years. Its biggest advantage compared to these sensors is its wider pH working range at both concentrations (1.0×10^{-2} and 1.0×10^{-3} M). As a result, the newly developed sensor is similar in some parameters and superior in others when compared to other copper(II) selective sensors.

Conclusion

In this study, a new copper(II)-selective potentiometric sensor was developed. The surface of this developed sensor was analyzed by SEM after conditioning it in copper(II) solution. The results obtained show that copper(II) ions are attached to the gaps on the sensor surface and are homogeneously distributed on the entire surface. This result shows that the ionophore can interact with copper(II) ions. The proposed sensor had Nernstian response, low detection limit, fast response time and good selectivity. In addition, it was repeatable and stable. The newly developed sensor was applied in real samples and detected Cu(II) ions with high recoveries.

Acknowledgements The authors would like to thank Dr. Caglar Berkel and Lecturer Serkan Ören for their contributions.

Declarations

Conflict of interest The authors declare that there is no conflict of interest.

References

1. W. Zhang, J. Li, W. Qin, Talanta **258**, 124444 (2023). https://doi.org/10.1016/j.talanta.2023.124444
2. O. Özbek, S. Ören, M.B. Gürdere, Ö. Isildak, M. Ceylan, Chem. Pap. **77**, 6679–6687 (2023). https://doi.org/10.1007/s11696-023-02968-0
3. L. Qi, R. Liang, T. Jiang, W. Qin, TrAC. Trends Anal. Chem. **150**, 116572 (2022). https://doi.org/10.1016/j.trac.2022.11657
4. A.M. Hassan, K.M. Kelani, M.A. Hegazy, M.A. Tantawy, Anal. Chim. Acta **1278**, 341707 (2023). https://doi.org/10.1016/j.aca.2023.341707
5. G. Cui, R. Liang, W. Qin, Anal. Chim. Acta **1239**, 340720 (2023). https://doi.org/10.1016/j.aca.2022.340720
6. C.R. Rousseau, P. Bühlmann, TrAC. Trends Anal. Chem. **140**, 116277 (2021). https://doi.org/10.1016/j.trac.2021.116277
7. I.M. Mostafa, C. Meng, Z. Dong, B. Lou, G. Xu, Anal. Sci. **38**, 23–37 (2022). https://doi.org/10.2116/analsci.21SAR02
8. J. Briffa, E. Sinagra, R. Blundell, Heliyon **6**, e04691 (2020). https://doi.org/10.1016/j.heliyon.2020.e04691
9. M.N. Kopylovich, K.T. Mahmudov, A.J. Pombeiro, J. Hazard. Mater. **186**, 1154–1162 (2011). https://doi.org/10.1016/j.jhazmat.2010.11.119
10. C. Topcu, G. Lacin, V. Yilmaz, F. Coldur, B. Caglar, O. Cubuk, I. Isildak, Anal. Lett. **51**(12), 1890–1910 (2018). https://doi.org/10.1080/00032719.2017.1395035
11. O. Özbek, M.B. Gürdere, C. Berkel, Ö. Isildak, J. Electrochem. Sci. Technol.Electrochem. Sci. Technol. **14**, 66–74 (2023). https://doi.org/10.33961/jecst.2022.00661
12. O. Özbek, Ö. Isildak, J. Chin. Chem. Soc. **69**, 1060–1069 (2023). https://doi.org/10.1002/jccs.202200168
13. G.J. Brewer, J. Trace Elem. Med. Biol. **26**, 89–92 (2012). https://doi.org/10.1016/j.jtemb.2012.04.019
14. A.A. Taylor, J.S. Tsuji, M.R. Garry, M.E. McArdle, W.L. Goodfellow, W.J. Adams, C.A. Menzie, Environ. Manag. **65**, 131–159 (2020). https://doi.org/10.1007/s00267-019-01234-y
15. V.K. Gupta, A.K. Jain, G. Maheshwari, H. Lang, Z. Ishtaiwi, Sens. Actuators B Chem. **117**, 99–106 (2006). https://doi.org/10.1016/j.snb.2005.11.003
16. W. Zeng, Y. Chen, H. Cui, F. Wu, Y. Zhu, J.S. Fritz, J. Chromatogr. A **1118**, 68–72 (2006). https://doi.org/10.1016/j.chroma.2006.01.065
17. F. Zhou, C. Li, H. Zhu, Y. Li, Optik **182**, 58–64 (2019). https://doi.org/10.1016/j.ijleo.2018.12.159
18. V. Kaur, A.K. Malik, Ann. Chim. **97**, 1279–1290 (2007). https://doi.org/10.1002/adic.200790113
19. V. Yılmaz, Ş Kartal, Int. J. Environ. Anal. Chem. **95**, 106–120 (2015). https://doi.org/10.1080/03067319.2014.994614
20. R.M. Alghanmi, J. Chem. **9**, 1007–1016 (2012). https://doi.org/10.1155/2012/279628
21. O. Özbek, Ö. Isildak, Bull. Mater. Sci. **45**, 114 (2022). https://doi.org/10.1007/s12034-022-02696-3
22. O. Özbek, H. Gezegen, A. Cetin, Ö. Isildak, ChemistrySelect **7**, e202202494 (2022). https://doi.org/10.1002/slct.202202494
23. A.M. Paredes, Microscopy | Scanning Electron Microscopy ed. by C.A. Batt, M.L. Tortorello, Encyclopedia of Food Microbiology (Elsevier, 2014), pp. 693–701. https://doi.org/10.1016/B978-0-12-384730-0.00215-9
24. A.E. Ali, A.A. Abbas, G.G. Mohamed, Microchem. J. **184**, 108178 (2023). https://doi.org/10.1016/j.microc.2022.108178
25. R.G. Deghadi, A.S. Eliwa, A.E. Ali, W.M. Hosny, G.G. Mohamed, Comments Inorg. Chem. **41**, 189–212 (2021). https://doi.org/10.1080/02603594.2020.1870963
26. I. Isildak, M. Yolcu, O. Isildak, N. Demirel, G. Topal, H. Hosgoren, Microchim. Acta **144**, 177–181 (2004). https://doi.org/10.1007/s00604-003-0072-7
27. O. Özbek, J. Food Compos. Anal. **115**, 104937 (2023). https://doi.org/10.1016/j.jfca.2022.104937
28. R.P. Buck, E. Lindner, Pure Appl. Chem. **66**, 2527–2536 (1994). https://doi.org/10.1351/pac199466122527
29. Y.A. Mohammed, A.A. Abbas, M.E.B. Mohamed, Appl. Organomet. Chem. **37**, e7156 (2023). https://doi.org/10.1002/aoc.7156
30. Y. Umezawa, P. Bühlmann, K. Umezawa, K. Tohda, A.S. Amemiya, Pure Appl. Chem. **72**, 1851–2082 (2000). https://doi.org/10.1351/pac200072101851
31. M.A. Abu-Dalo, A.A. Salam, N.S. Nassory, Int. J. Electrochem. Sci. **10**, 6780–6793 (2015). https://doi.org/10.1016/S1452-3981(23)06761-5
32. B. Hasani, A. Zamani, M.K. Moftakhar, M. Mostafavi, M.R. Yaftian, M. Ghorbanloo, J. Anal. Chem. **71**, 82–90 (2018). https://doi.org/10.1134/S1061934818010021
33. N. Aslan, Z. Koçak, H. KormalıErtürün, N. Şen, Anal. Bioanal. Chem. Res. **10**, 193–204 (2023)
34. L. Xu, S. Gan, L. Zhong, Z. Sun, Y. Tang, T. Han, L. Niu, J. Electroanal. Chem. **904**, 115923 (2022). https://doi.org/10.1016/j.jelechem.2021.115923
35. O. Özbek, A. Ölcenoglu, Microchem. J. **190**, 108679 (2023). https://doi.org/10.1016/j.microc.2023.108679